Self-Consistent Boundary Conditions in the 2D *XY* Model

Peter Olsson
Department of Theoretical Physics, Umeå University, 901 87 Umeå, Sweden
(Received 31 August 1994)

A generalization of periodic boundary conditions to incorporate fluctuations with wavelength larger than the system size is discussed. These boundary conditions are applied to Monte Carlo calculations on the two-dimensional *XY* model. The finite-size effect on the vortex-vortex correlation function, and thereby the dielectric function, is shown to be virtually eliminated. These Monte Carlo data are shown to be in excellent agreement with the Kosterlitz renormalization group equations, and the critical temperature is found to be $T_c = 0.8922(2)$.

PACS numbers: 05.50.+q, 64.60.Fr, 75.10.Hk, 75.40.Cx

Monte Carlo (MC) simulations together with finite size scaling have proven to be flexible and powerful tools for the analysis of model systems in statistical physics. The behavior in the thermodynamic limit may often be extracted through analysis of the size dependence of various quantities. In these cases periodic boundary conditions (PBC) seem to be both a natural and an ideal choice. The periodic boundary conditions are, however, not ideally suited for determinations of spatial correlations, as, e.g., the spin-spin correlation function. Because of the periodicity, reliable results for such quantities are obtained only for distances much smaller than the size of the lattice.

For determinations of that kind of quantities, one would ideally have the finite simulated system embedded into an infinite one, since that would eliminate all finite-size effects. While that is impracticable, we see that a major difference between such an embedded system and a system with ordinary PBC would be the presence of fluctuations with wavelength larger than the size of the system. The main ideas of the present paper are therefore, first, to generalize the PBC to incorporate long-wave fluctuations and, second, to take due account of the effect of the imagined surrounding to optimally tune the amplitude of these fluctuations. We will, specifically, show how this may be accomplished for a system with a continuous degree of freedom—the two-dimensional (2D) *XY* model.

The 2D *XY* (planar rotator) model is defined by the Hamiltonian

$$H = -J\sum_{\langle ij\rangle}\cos(\theta_i - \theta_j),$$

where i and j enumerate the lattice sites, θ_i is an angle associated with site i, and the sum is over nearest neighbors. The 2D *XY* model undergoes a Kosterlitz-Thouless transition [1,2] which at a square lattice, the case discussed in the present Letter, takes place at $T_c \approx 0.89J$ [3–8].

In this model the helicity modulus Y is a candidate for finite size scaling. Hyperscaling implies that Y obeys the Josephson relation and at criticality scales as L^{2-d} [9], where L is the system size and d is the dimension. This approach works well in analyses of MC data in three dimensions [9] but is not useful for $d = 2$. This is because Y in two dimensions approaches a constant logarithmically; the approach is therefore exceedingly slow. One can, however, improve the situation considerably by making use of some knowledge of the approach to this constant, from Kosterlitz' renormalization group (RG) equations.

To facilitate a comparison between the predictions from the RG equations and MC data, we need to determine the dielectric function $\epsilon_t(k)$ [1]. This is therefore the central quantity in the present Letter. The dielectric function is directly related to the effective vortex interaction, which below T_c is logarithmic for all r, and at $T \to 0$ is given by [1]

$$V(r) \sim -2\pi J \ln r \Leftrightarrow V(\mathbf{k}) = -4\pi^2 J G(\mathbf{k}),$$

where $G(\mathbf{k}) = (2\cos k_x + 2\cos k_y - 4)^{-1}$ is the lattice Green's function. The dielectric function describes how $V(\mathbf{k})$ is reduced from this zero-temperature result:

$$V(\mathbf{k}) = -\frac{4\pi^2 J G(\mathbf{k})}{\epsilon_t(\mathbf{k})}.$$

It turns out that $1/\epsilon_t(\mathbf{k})$ may be expressed in terms of the correlation function [10]

$$\frac{J}{\epsilon_t(\mathbf{k})} = \frac{J_0}{\epsilon(\mathbf{k})} = J_0\left(1 - \frac{4\pi^2 J_0 G(\mathbf{k})}{TL^2}\langle n(\mathbf{k})n(-\mathbf{k})\rangle\right), \quad (1)$$

where $J_0 = \langle\cos(\theta_i - \theta_j)\rangle$ is the contribution from the spin waves, L^2 is the number of lattice points, and $n(\mathbf{k})$ is the Fourier transform of the vorticity distribution [10]. We use $1/\epsilon_t(k)$ for the quantity that contains contributions from both spin waves and vortices, in contrast to $1/\epsilon(k)$ that solely contains the effect of the vorticity, i.e., the rotation of the current [10].

Monte Carlo results for the dielectric function in a system with PBC are shown by the symbols above the dividing line in Fig. 1. The data are for $T = 0.89J$ (close to T_c) and four different lattice sizes, $L = 8$, 16, 32, and 64. The finite-size effect is very pronounced; $1/\epsilon_t$ for constant k *decreases* with increasing lattice size. The MC

0031-9007/94/73(25)/3339(4)$06.00

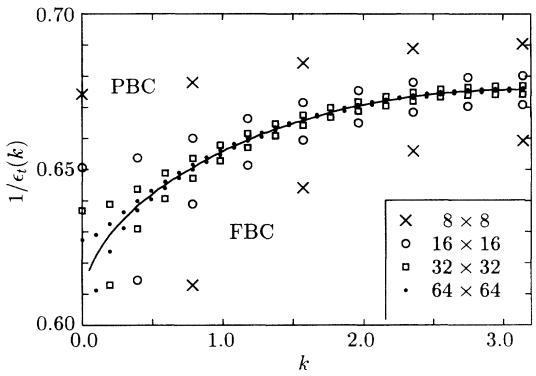

FIG. 1. Shown are MC data for periodic and fluctuating boundary conditions at $T = 0.89J$, close to T_c. For PBC (points above the solid line) $1/\epsilon_t$ *decreases* with increasing lattice size, whereas it *increases* for FBC (points below the solid line). The solid line is the common limiting function as $L \to \infty$. The statistical uncertainties are smaller than the size of the symbols.

simulations are done with Wolff's cluster update method [11], with typically 2×10^6 update sweeps on the largest lattices.

Since we like to introduce fluctuations with long wavelength, we then include twist variables Δ_x and Δ_y as another pair of dynamic variables. One may think of these variables as being situated at the respective boundaries of the system, such that the angular difference across the boundaries become $\theta_{L,y} + \Delta_x - \theta_{L,y}$ and $\theta_{x,L} + \Delta_y - \theta_{x,1}$ for the respective directions. This is the definition of the fluctuating boundary conditions (FBC).

For most purposes it is, however, convenient to spread these twists over the whole system instead of keeping them at the boundary. This is done with the substitution $\theta_i \to \theta_i + \mathbf{r}_i \cdot \boldsymbol{\Delta}/L$, where $\boldsymbol{\Delta} = (\Delta_x, \Delta_y)$. The angular difference then becomes

$$\theta_i - \theta_j \quad \to \quad \theta_i - \theta_j + \mathbf{r}_{ij} \cdot \boldsymbol{\Delta}/L,$$

where $\mathbf{r}_{ij}$ is a unit vector from site j to i.

The symbols in the lower part of Fig. 1 are MC data from simulations with fluctuating boundary conditions. Note that the finite-size effect in this case is the opposite to what was found for PBC; the values *increase* with increasing lattice size. This is due to the too large amplitude of the twist fluctuations, which causes too large fluctuations for all $\mathbf{k}$.

In these simulations the update of the Δ variables was done with the ordinary Metropolis algorithm whereas the spin variables $\{\theta_i\}$ were handled with Wolff's cluster update algorithm. The cluster update works well as long as the clusters do not close after crossing the boundary. In that case the cluster becomes invalid, and the previous configuration has to be restored [12]. Even though a large portion of the time was wasted on such clusters that eventually grew too large, the cluster update in our comparisons was considerably more efficient than the ordinary Metropolis algorithm.

In view of the two sets of symbols in Fig. 1, one would expect a reduced amplitude in the Δ fluctuations to give smaller finite-size effects in the MC simulations. Considering the $L \times L$ system in our simulation as being embedded in an infinite surrounding medium, this amounts to taking the stiffness of this medium against the twist fluctuations into account. The amplitude may be controlled by including a second term in the Hamiltonian,

$$H = -J \sum_{\langle ij \rangle} \cos(\theta_i - \theta_j + \mathbf{r}_{ij} \cdot \boldsymbol{\Delta}/L) + \mu \left(\frac{\Delta_x^2}{2} + \frac{\Delta_y^2}{2} \right).$$

By adjusting μ we may go continuously from periodic to fluctuating boundary conditions, $\mu = \infty$ to 0. We now address the question how μ should be chosen, to mimic the behavior of the surrounding medium in the best possible way.

In the zero-temperature limit, the amplitudes of the twist fluctuations fulfill [10]

$$\frac{T}{\langle \Delta^2 \rangle} = J + \mu,$$

which shows that there are two terms that restrain the twist fluctuations; the total stiffness against the twists is the sum of the stiffness of the system itself, and the stiffness of the surrounding medium.

At general temperatures we make use of a similar expression to define the *internal stiffness* $\tilde{\Upsilon}$ [13], which depends on temperature, lattice size, and μ,

$$\frac{T}{\langle \Delta^2 \rangle} = \tilde{\Upsilon} + \mu.$$

We may now consider the surrounding medium as being made up of a huge number of $L \times L$ blocks, each with the internal stiffness $\tilde{\Upsilon}$. It is then possible to show that μ, the combined effect of these blocks to resist the twists in the system, is equal to the stiffness of a single block [12]. One therefore arrives at the self-consistent condition

$$\tilde{\Upsilon} = \mu, \tag{2}$$

which characterizes the self-consistent boundary conditions (SCBC). The data in Fig. 2, obtained by means of Eq. (2), show that this choice gives considerably reduced finite-size effects; *the finite-size effect is virtually eliminated.* The data are for lattices with $L = 8$, 16, 32, and 64, at $T/J = 0.89$. The same reduction of the finite-size effect holds for all temperatures below and closely above T_c.

Instead of adjusting μ in the MC simulations to precisely the correct value, the simulations were done with two different μ, close to the (unknown) self-consistent value. The desired data were obtained by linear interpolation. As an example, $1/\epsilon_t(k)$ in Fig. 2 is from simulations with $\mu/J = 0.55$ and 0.60. The self-consistent values of μ for the different system sizes were determined to be $\mu/J = 0.6010$, 0.5865, 0.5769, and 0.5761 for $L = 8$, 16, 32, and 64.

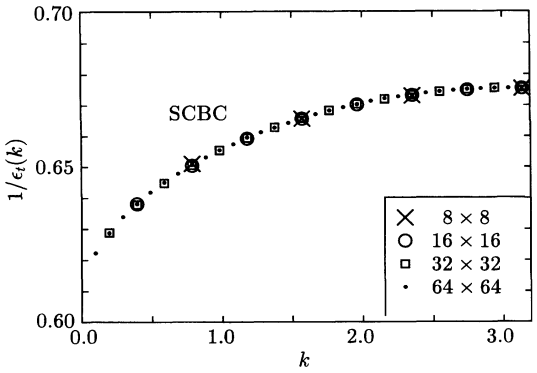

FIG. 2. The dielectric function obtained with self-consistent boundary conditions, Eq. (2), at $T/J = 0.89$. The finite-size effect is virtually eliminated.

We now turn to a comparison between our self-consistently obtained data for $1/\epsilon_t(k)$ and the behavior prescribed by Kosterlitz's RG equations. From the RG equations [2], the behavior of the length-dependent dielectric constant $1/\epsilon_t(\ell)$ around the critical line is given by [14]

$$\frac{J\pi}{2\epsilon_t(\ell)T} = 1 + c\coth[2c(\ell + \ell_0)], \qquad T < T_c, \quad (3a)$$

$$\frac{J\pi}{2\epsilon_t(\ell)T} = 1 + [2(\ell + \ell_0)]^{-1}, \qquad T = T_c, \quad (3b)$$

$$\frac{J\pi}{2\epsilon_t(\ell)T} = 1 - c\cot[2c(\ell_0 - \ell)], \qquad T > T_c, \quad (3c)$$

where ℓ is a logarithmic length scale, and c and ℓ_0 are fitting parameters.

Figure 3 shows the result of fitting MC data for $1/\epsilon_t(k)$ by Eqs. (3). The solid lines are $1/\epsilon(\ell)$, given by Eqs. (3). The open circles are MC data at six different temperatures. The fitting parameters are shown in Table I. The thick line is for the critical trajectory, and the corresponding MC data for the temperature $T_c/J = 0.8922(2)$. The lines above and below the thick line are for lower and higher temperatures, respectively.

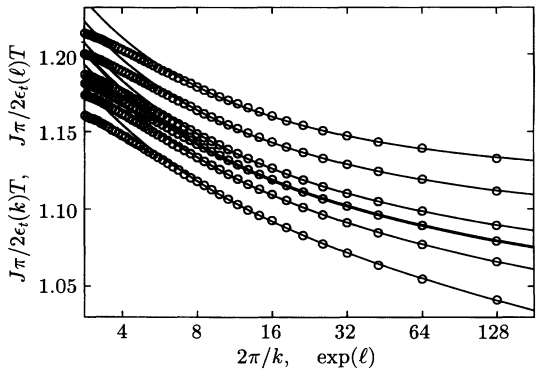

FIG. 3. Fitting of the self-consistently obtained $1/\epsilon_t$ (open circles) to $1/\epsilon_t(\ell)$ from Eqs. (3) (solid lines) at six different temperatures, $T/J = 0.880$, 0.885, 0.890, 0.89218, 0.895, and 0.900. The thick line corresponds to the critical trajectory and Eq. (3b). The errors in the MC data are smaller than the size of the symbols, cf. Table II.

TABLE I. Results from fitting MC data for $1/\epsilon_t(k)$, obtained with SCBC, to Eqs. (3).

T/J	c	ℓ_0	χ^2/DOF	Fit by Eq.
0.880	0.12028	1.309	1.32	(3a)
0.885	0.09087	1.362	1.37	(3a)
0.890	0.04918	1.417	1.44	(3a)
0.892	0.01414	1.441	1.41	(3a)
0.89218		1.443	1.41	(3b)
0.893	0.02972	51.40	1.39	(3c)
0.895	0.05473	27.22	1.37	(3c)
0.900	0.08910	16.08	1.48	(3c)

The fits are excellent down to wavelengths $2\pi/k \approx 7$ but break down at smaller lengths. This is also expected for two different reasons. First, the RG equations are only reliable for small fugacities, which implies large length scales. Second, the lattice structure has an effect on the behavior of the XY model at small distances, which is not included in the RG equations.

The actual fitting was done with five evenly spaced values of $\ln(2\pi/k)$, corresponding to wavelengths $2\pi/k = 8$, 16, 32, 64, and 128. To obtain best possible precision in the fits, the MC data at several temperatures in a narrow interval, $0.87 \le T \le 0.90$, were first fitted by a second order polynomial in $\tau = T/J - 0.89$,

$$\frac{J\pi}{2\epsilon_t(k)T} = \alpha_k + \beta_k\tau + \gamma_k\tau^2. \quad (4)$$

The obtained parameters, which are shown in Table II, were then employed to determine our values of $1/\epsilon_t(k)$ to be used in the fits.

From the data in Table I it is possible to extract some nonuniversal constants pertinent to the KT transition in the 2D XY model. One such constant is the slope B in the behavior of the characteristic length as $T \to T_c^+$ [2],

$$\ln\xi = \text{const} + \frac{B}{\sqrt{T/T_c - 1}}. \quad (5)$$

With $\ln\xi \equiv \ell_0$ for $T > T_c$ in Table I, this behavior is obeyed to an excellent approximation with $B \approx 1.585(9)$.

TABLE II. Parameters from fits by Eq. (4).

$2\pi/k$	α_k	β_k	γ_k
8	1.14844(15)	−3.04(2)	−1.6
16	1.12637(17)	−3.38(2)	−1.9
32	1.11005(19)	−3.79(3)	−7.6
64	1.09853(22)	−4.23(3)	−16.7
128	1.08941(25)	−4.57(4)	−24.2

A detailed comparison with previous results will be given elsewhere [12].

Several authors have performed the same kind of fits to predictions from the Kosterlitz RG equations, with the size dependence of the helicity modulus $\Upsilon = J/\epsilon_t(0)$ instead of the length dependence of $1/\epsilon_t$, both for the critical trajectory [3,4] and for some trajectories below T_c [5]. The underlying assumption is that the *size* dependence in Υ directly reflects the *length* dependence in $1/\epsilon_t$. As shown in Fig. 4, this is, however, not correct for the typical lattice sizes used in these analyses. The figure shows a comparison between these two quantities; the factor $g \approx 1.70$ is chosen to give agreement at large lengths.

The solid squares in Fig. 5 show the difference in Fig. 4 in more detail. With a proper adjustment of the factor g, the difference vanishes algebraically, $\sim L^{-1.79}$. Also shown is the approach to the thermodynamic limit of $1/\epsilon_t(k = \pi/4, L)$ with PBC, cf. Fig. 1.

In conclusion, we have generalized the periodic boundary conditions to include fluctuations larger than the system size and controlled the amplitude of these fluctuations in a self-consistent way. With this idea applied to MC simulations of the 2D XY model, the finite-size effect in the dielectric function is virtually eliminated. The obtained dielectric function is shown to be in excellent agreement with results from Kosterlitz's RG equations; we specifically find $T_c/J = 0.8922(2)$. It is also shown that the *size* dependence of Υ differs significantly from the *length* dependence of $1/\epsilon(k)$ for most commonly used lattice sizes.

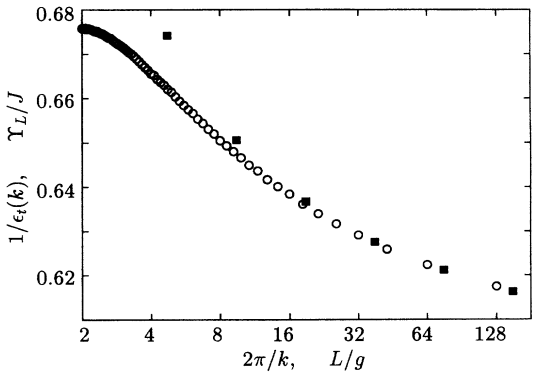

FIG. 4. Size-dependence of the helicity modulus, $L = 8 \ldots 256$ (determined with PBC), together with the length dependence of the dielectric function (SCBC, $L = 128$) at $T = 0.89J$. At large lengths these two quantities agree, but at sizes $L \lesssim 64$ the difference becomes significant.

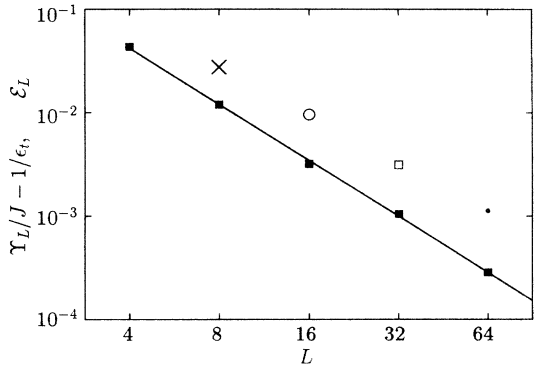

FIG. 5. The solid squares are the difference between corresponding values of Υ and (interpolated values of) $1/\epsilon_t$ in Fig. 4. Also shown is the approach to the thermodynamic limit for $1/\epsilon_t(k = \pi/4, L)$ with PBC. The notation used is $\mathcal{E}_L = 1/\epsilon_t(\pi/4, L) - 1/\epsilon_t(\pi/4, \infty)$.

The author thanks Mats Nylén for stimulating discussions and Professor Petter Minnhagen and Mats Wallin for critical reading of the manuscript. Financial support from the Swedish Natural Research Council through Contract No. E-EG 10376-302 is gratefully acknowledged.

[1] J. M. Kosterlitz and D. J. Thouless, J. Phys. C **6**, 1181 (1973).
[2] J. M. Kosterlitz, J. Phys. C **7**, 1046 (1974).
[3] H. Weber and P. Minnhagen, Phys. Rev. B **37**, 5986 (1988).
[4] P. Olsson and P. Minnhagen, Phys. Scr. **43**, 203 (1991).
[5] N. Schultka and E. Manousakis, Phys. Rev. B **49**, 12 071 (1994).
[6] J. Tobochnik and G. Chester, Phys. Rev. B **20**, 3761 (1979).
[7] R. Gupta and C. F. Baillie, Phys. Rev. B **45**, 2883 (1992).
[8] P. Butera and M. Comi, Phys. Rev. B **47**, 11 969 (1993).
[9] M.-C. Cha *et al.*, Phys. Rev. B **44**, 6883 (1991).
[10] P. Olsson, Phys. Rev. B **46**, 14 598 (1992).
[11] U. Wolff, Phys. Rev. Lett. **62**, 361 (1989).
[12] P. Olsson (unpublished).
[13] The internal stiffness $\tilde{\Upsilon}$ is not the same as the helicity modulus Υ, which, by the way, is useful only with periodic boundary conditions.
[14] P. Minnhagen, Rev. Mod. Phys. **59**, 1001 (1987).